This article has been accepted for publication in a future issue of this journal, but has not been fully edited. Content may change prior to final publication. Citation information: DOI 10.1109/TPEL.2015.2456155, IEEE Transactions on Power Electronics

A Robust LQG Servo Control Strategy of Shunt Active Power Filter for Power Quality Enhancement

R. Panigrahi, B. Subudhi, *Senior Member, IEEE* and P.C. Panda, *Senior Member, IEEE*

***Abstract*— This paper proposes a Linear Quadratic Gaussian (LQG) Servo controller for the current control of Shunt Active Power Filter (SAPF) operating under balanced and unbalanced supply voltages. This LQG controller is comprised of a LQ regulator and a Kalman filter (KF) that minimizes the error between the output currents and their variations. A feedback compensator is used in LQG Servo controller that benefits a SAPF system by increasing tracking error reduction, gain stability, reducing amplitude distortion and sensitivity to external disturbances. A Kalman filter based new reference current generation scheme is developed here to resolve the difficulty of tuning gains of a proportional integral (PI) controller and for avoiding the use of voltage sensors making it cost effective. Consequently, this reference scheme has self-capability of dc-link voltage regulation by adaptively estimating the peak value of source reference current with changing load conditions. The control algorithm is embedded in SAPF using a MATLAB/Simulink software environment. The effectiveness of the proposed LQG Servo_{KF} algorithm is evaluated through comparison with an existing LQR_{KF} algorithm and then validated with experimental studies pursued using a dSPACE1104 computing platform. From the obtained experimental and simulation results it is observed that the proposed control strategy exhibits superior performance in terms of robustness improvement and current harmonics mitigation under steady-state and dynamic load conditions, thus making it more effective for practical applications.**

***Index Terms*— Linear Quadratic Gaussian (LQG), Kalman filter, Feedback compensator, Measurement noise, Reference current, Robustness**

I. Introduction

Electrical power quality [1], [2] has been a growing concern because of the proliferation of the nonlinear loads, which causes significant increase of line losses, instability and voltage distortion. With injection of harmonic current into the system, these nonlinear loads additionally cause low power factor. The resulting unbalanced current adversely affects every component in the power system and equipment. This results in poor power factor, increased losses, excessive neutral currents and reduction in overall efficiency. Although load compensation using passive filters is simple to design and operate, it has drawbacks such as resonance, detuning and overloading. Moreover, passive filter is not suitable for fast changing loads. The aforesaid issues can be effectively mitigated by employing a SAPF. The main issue related to the effective operation of a SAPF is its ability to compensate harmonics [3], reactive power, parametric uncertainties of load, supply unbalance and point of common coupling (PCC) voltage distortion.

Various control schemes have been applied in SAPF [4], [5] under both balanced and unbalanced loading conditions. However, these control strategies have not considered some important aspects of power system perturbations such as supply unbalance, variations in the SAPF as well as load parameters and grid perturbations such as measurement noise and voltage distortion. Further, due to parametric uncertainties present in the load, the problem of compensating the SAPF becomes more complicated which adversely effects towards its satisfactory operation. A linear quadratic control combined with an integral control has been employed to control a three phase three wire SAPF to achieve unity power factor at PCC of a heavily distorted and unbalanced load currents [6]. This control uses the full state vector available for feedback, but this is unrealistic as there is always a measurement noise. An optimal control theory [7] supported LQR and KF was proposed considering measurement noise, load currents and grid voltage transients. However PCC voltage has not been considered as a disturbance in the SAPF model. LQR law is based on the availability of the complete state vector, which may not be completely measurable in most of the real-world situations. To overcome this, a LQG servo controller was proposed for voltage source converter (VSC) connected to the grid [8], where KF was employed to estimate the state vector. In this case, power system perturbations have not been taken into consideration and also the presence of a time delay at the reference tracking point gives rise to a slow response of the overall system. Thus, tracking error is not reduced effectively and stability of the system is minimally improved. However, a fast response without any tracking error delay is indispensable for a SAPF system so that efficient current harmonics compensation can be achieved under aforementioned perturbations. To resolve the above issues, in the present paper, a modification of above LQG servo controller has been performed by employing a suitable feedback compensator having gain of $-(1/2)$, which has the capability of fast increasing tracking error reduction of the SAPF system by rejecting all types of perturbations raised in source and load areas. The idea behind this feedback compensator is to achieve gain stability, perfect tracking, and less current harmonics distortion.

Another important aspect of SAPF is the reference current generation, which ensures capacitor voltage regulation [9] under all types perturbations occurred in source and load sides and this voltage regulation is achieved by adjusting a small

Authors are with the Department of Electrical Engineering, National Institute of Technology, Rourkela, 769008, Odisha.(e-mail: rpanigrahi99@gmail.com, bidyadhar@nitrkl.ac.in, pcpanda1948@gmail.com)

This article has been accepted for publication in a future issue of this journal, but has not been fully edited. Content may change prior to final publication. Citation information: DOI 10.1109/TPEL.2015.2456155, IEEE Transactions on Power Electronics

amount of real power flowing through shunt inverter into the dc link capacitor. Further, this small amount of real power is adjusted by changing the peak value of the reference current. A PI controller [10] is normally used for determining this peak value of reference current and its performance is satisfactory up to steady state level. But when load changes, the peak value of reference current must be adjusted quickly to proportionally change the real power drawn from the source to keep satisfactory operation of SAPF. In this fashion, dc voltage regulation is directly dependent upon the peak value of reference source current. With abovementioned views, our proposed source reference current scheme is based upon estimation of the desired peak value of reference current adaptively employing KF, as a consequence capacitor voltage regulation is very fast with consideration of power system perturbations arisen in load as well as source sides.

It is not possible to supply quality power to the special equipment e.g. programmable logic controller (PLC), distributed control system (DCS), converters in AC drives through conventional control schemes [6]-[8], [11] employed in SAPF. This results in malfunctioning of the above type of equipment, which need pure power at all moments with fast changing disturbances occurred in the power system. Hence a fast and robust control action is necessary to supply pure and distortion less power to above equipment with all perturbations taken into account. In view of aforementioned issues, we focus on the development of robust LQG servo controller with a faster reference estimation scheme in SAPF, which permits all perturbations such as PCC voltage distortion, measurement noise, parametric variations of load, capacitor voltage and filter impedance, tracking error variations and supply voltage unbalance so that compensation capability of the overall SAPF system can be enhanced.

The paper is organized as follows. In section II, the configuration of SAPF model along with the hardware description are presented. Section III briefly explains the proposed reference generation scheme together with proposed LQG servo controller strategy used in SAPF. The results obtained from simulation studies using MATLAB and hardware implementations are presented and discussed for various cases of power system perturbations in section IV. Finally, the conclusion is presented in section V.

II. HARDWARE DESCRIPTION OF SAPF MODEL

The basic topology of a prototype SAPF developed in the laboratory prototype is presented in Fig. 1(a). This topology is composed of a voltage source inverter (VSI) connected to PCC through filter impedances (R_F, L_F). A nonlinear load comprising of a three phase diode bridge rectifier with RL load is considered. The control of SAPF is achieved by LQG servo controller based algorithm implemented with dSPACE1104. Firstly the controller is implemented using Simulink/MATLAB. The real time workshop is used to generate C code for real time applications. The interface between Simulink/MATLAB and dSPACE1104 permits running the control algorithm. The basic control structure and its mathematical equations are presented in section III. The switching signals generated from the slave DSP (TMS320F240) are fed to blanking circuit (integrated circuit of SN74LS123) and opto-isolation circuit (high speed opto-couplers ICHCPL2601). For implementation, the control

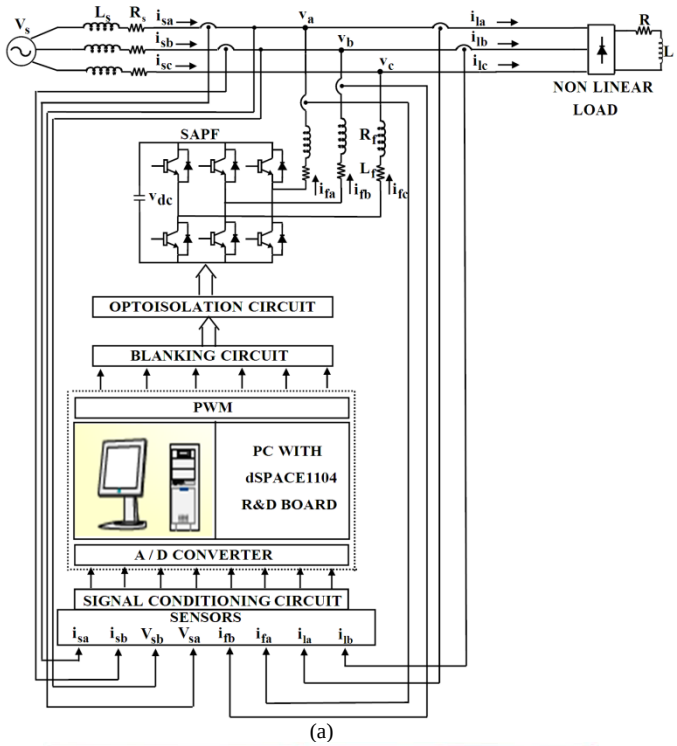

(a)

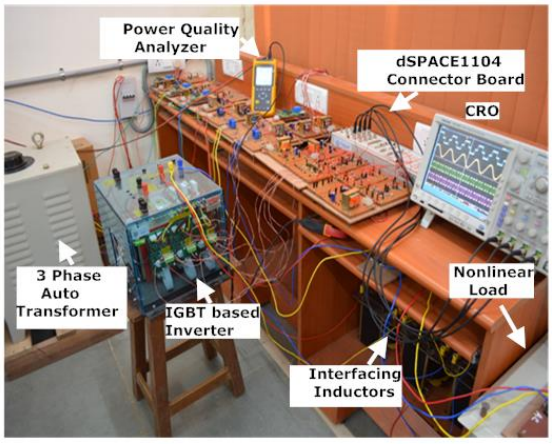

(b)

Fig.1 Hardware Details, (a) Block diagram of the control and power circuit of SAPF, (b) Experimental Set up

TABLE I
SYSTEM PARAMETERS USED FOR SIMULATION AND EXPERIMENT

System Parameter	Supply voltage RMS line-line (V_s)=100V Supply impedance (R_s = 0.1 Ω and L_s = 0.5 mH) Supply frequency (f)=50 Hz
Load	Nonlinear Load: 3-phase diode bridge rectifier with resistive load of impedance (R=20Ω and L=10 mH) (Base Case)
SAPF	DC link capacitor (C)=2350μF; Reference DC Link voltage (v_{dc}^*)=220V; Filter impedance (R_f = 0.05 Ω and L_f = 2.5 mH) Switching frequency (f_{sw}) =12.5 kHz Sampling frequency (f_s)=25 kHz
PI Controller	K_p = 0.32, K_i = 1

This article has been accepted for publication in a future issue of this journal, but has not been fully edited. Content may change prior to final publication. Citation information: DOI 10.1109/TPEL.2015.2456155, IEEE Transactions on Power Electronics

algorithm is run at a fixed step size of 78.125 µs and hence, the maximum switching frequency of VSC of SAPF is fixed at 12.8 kHz. The dead time for each leg of IGBT is set to 4 µs. The compensating currents (i_{fa}, i_{fb}) of phase 'a' and 'b' are sensed using Hall effect current sensors (LEM LA 55-P). Since it is a three wire system, phase 'c' current can be calculated as $i_{fc} = -(i_{fa} + i_{fb})$. Similarly the source currents and load currents for phase 'a' and 'b' are sensed. To sense the voltage signals of phase 'a' and 'b', two voltage sensors (LEM LV 25-P) are used. The design specifications and circuit parameters in laboratory prototype are given in Table I.

III. DEVELOPMENT OF CONTROL SYSTEM

We present the control algorithm in the development of SAPF in two distinct steps namely reference generation and current controller implementation, which are described subsequently as below.

A. Proposed Reference Current Generation Scheme

When load parameter varies, average voltage across the dc link capacitor deviates from its reference value and the real power supplied by the source is not enough to supply the load demand. The SAPF can't immediately respond to the load change since it takes a longer interval to calculate a new reference current. This drawback is overcome by the proposed reference scheme with a fast and adaptive estimation of peak value of source reference current, which has the capability of delivering real power equivalent to conduction and switching losses occurred during capacitor voltage deviation. As a result, it is expected that our proposed reference generation scheme can overcome the demerits of PI control and makes the dc link capacitor voltage steady at the set point. This reference estimation approach has merit in avoidance of voltage sensors, tuning problems and synchronisation circuits needed for hardware, hence it becomes cost effective.

The proposed scheme is based on source reference generation principle and the reference compensating currents i^*_{fabc} for three phases a, b, and c are generated by subtracting the source references i^*_{sabc} from the load currents i_{labc} as shown in Fig.2(a). Source reference current generation is implemented by the modulation of the estimated peak value of source current (I_{max}) with the estimated in phase fundamental components $(i_{p(abc)})$ of load currents in per unit value, equations of which are provided below.

$$i^*_{sabc} = I_{max} \times i_{p(abc)} \quad (1)$$

$$i^*_{fabc} = i_{labc} - i^*_{sabc} \quad (2)$$

For an accurate estimation of reference current, the unit template $i_{p(abc)}$ must be undistorted and this condition is met by Kalman filtering estimation algorithm.

a. Formulation of KF algorithm for reference current generation

A linear signal z_k of single sinusoid is represented by

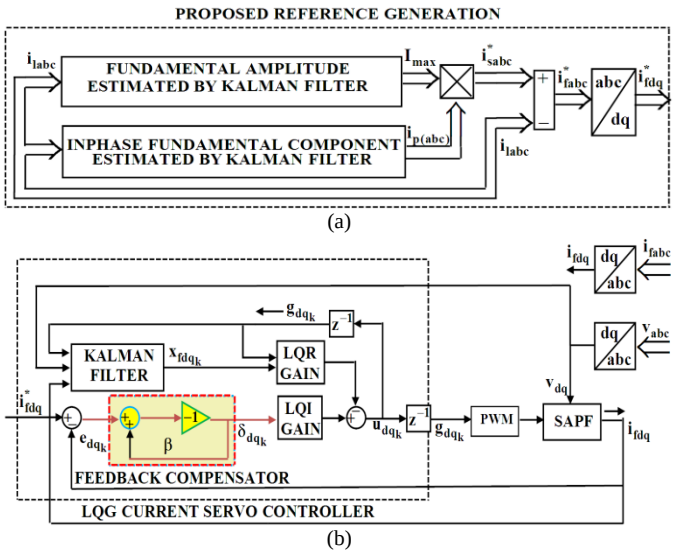

Fig.2 Proposed Control Structure, (a) Proposed Reference Generation Scheme, (b) Proposed LQG Servo Current Controller Strategy

$$z_k = a_1 \sin(k\omega_1 T_s + \phi_1) \quad k = 1, ..., N \quad (3a)$$

$$\omega_1 = 2\pi f_1 \quad (3b)$$

In eq (3), T_s denotes the sampling time, parameters a_1 and f_1 are the fundamental amplitude and frequency respectively with initial phase ϕ_1. The signal z_{k+1} can be expressed as

$$z_{k+1} = x_{1_{k+1}} = x_{1_k} \cos(k\omega_1 T_s) + x_{2_k} \sin(k\omega_1 T_s) \quad (4)$$

Further,

$$x_{2_{k+1}} = -x_{1_k} \sin(k\omega_1 T_s) + x_{2_k} \cos(k\omega_1 T_s) \quad (5)$$

where x_{2_k} is known as the in quadrature component and is orthogonal to x_{1_k} and they are represented by

$$x_{1_k} = a_1 \sin(k\omega_1 T_s + \phi_1) \quad (6a)$$

$$x_{2_k} = a_1 \cos(k\omega_1 T_s + \phi_1) \quad (6b)$$

To model amplitude or phase variations of the signal, a perturbation vector $[\gamma_1 \quad \gamma_2]^T_k$ in the system states is considered with the state space representation as

$$x_{k+1} = \Phi_k x_k + w_k \quad (7)$$

$$y_k = H_k x_k + v_k \quad (8)$$

where w_k and v_k are the process and measurement noises respectively and the state transition matrix Φ_k and the observed value H_k are given below.

$$\Phi_k = \begin{bmatrix} \cos(\omega_1 T_s) & \sin(\omega_1 T_s) \\ -\sin(\omega_1 T_s) & \cos(\omega_1 T_s) \end{bmatrix} \quad (9)$$

$$H_k = [1 \quad 0] \quad (10)$$

Denoting the estimate of x_{k+1} as $\hat{x}_{k+1|k}$, the sequential recursive computation steps for fundamental component identification are given by

$$\hat{x}_{k+1|k} = \Phi_k \hat{x}_{k|k-1} + K_k (y_k - H_k \hat{x}_{k|k-1}) \quad (11)$$

where

$$K_k = \Phi_k P_{k|k-1} H^T_k \left(H_k P_{k|k-1} H^T_k + R_{m_k} \right)^{-1} \quad (12)$$

This article has been accepted for publication in a future issue of this journal, but has not been fully edited. Content may change prior to final publication. Citation information: DOI 10.1109/TPEL.2015.2456155, IEEE Transactions on Power Electronics

is the Kalman gain and the error covariance matrix is given below.

$$P_{k+1|k} = \Phi_k P_{k|k-1} \Phi_k^T - K_k H_k P_{k|k-1} \Phi_k^T + Q_{m_k} \quad (13)$$

Q_{m_k} and R_{m_k} are the process and measurement error covariance matrix respectively.

$$P_{k+1|k} = E\{(x_{k+1} - \hat{x}_{k+1|k})(x_{k+1} - \hat{x}_{k+1|k})^T\} \quad (14)$$

$$Q_{m_k} = E\{w_k w_k^T\} \quad (15)$$

$$R_{m_k} = E\{v_k v_k^T\} \quad (16)$$

Based on the above estimates ($\hat{x}_{1_{k|}}$ and $\hat{x}_{2_{k|}}$), the fundamental component's magnitude [12] is calculated as follows,

$$I_{max} = \sqrt{\hat{x}_{1k}^{\ 2} + \hat{x}_{2k}^{\ 2}} \quad (17)$$

The in phase fundamental component with per unit value $(i_{p(abc)})$ can be expressed as

$$i_{p(abc)} = \sin\left(k\omega_1 T_s + \phi_1\right) = \frac{\hat{x}_{1_{k|}}}{I_{max}} \quad (18)$$

B. Proposed LQG Servo Current Controller

In the proposed LQG Servo controller, we consider a trade off but regulation/tracking performance and the control effort considering both process disturbances and measurement noise. We present next the design of our proposed LQG Servo controller.

a. Design of Proposed Feedback Compensator

The proposed feedback compensator plays a significant role in achieving gain stability, perfect reference tracking, less current harmonics distortion as well as improved bandwidth. Referring Fig. 2(b), the output of feedback compensator is expressed by the following equation.

$$\delta_{dq_k} = e_{dq_k} \times \beta \quad (19)$$

where β is the gain of feedback compensator and the corresponding gain value is determined as $(-1/2)$. e_{dq_k} is the tracking error of SAPF system and can be represented as

$$e_{dq_k} = i^*_{fdq_k} - i_{fdq_k} \quad (20)$$

where i_{fdq} is the dq transformation of compensating current i_{fabc}.

b. Construction of Kalman State Estimator

KF is used for measurement of harmonics [13], detection of grid perturbations [14] and estimation of fundamental component as well as system variables [15]. For linear systems contaminated with additive noise, KF is found to be an optimum estimator. In this paper, we need Kalman state estimator for LQG Servo control because we cannot implement LQ optimal state feedback without full state measurement.

For implementation of the KF, one inherent computational delay is considered within the switch input u_{dq} to the SAPF system due to finite computation time and PCC voltage v_{dq} also acts as an input to the estimator. The linear discrete-time system in dq frame can be represented as

$$\begin{aligned} x_{fdq_{k+1}} &= G_f x_{fdq_k} + S_f u_{fdq_k} + w_{f_k} \\ y_{fdq_k} &= C_f x_{fdq_k} + v_{f_k} \end{aligned} \quad (21)$$

where w_{f_k} and v_{f_k} are modeled as white noise and the associated noise covariance matrices are given by W_f and V_f .

Further,

$$x_{fdq_k} = \begin{bmatrix} i_{fd_k} & i_{fq_k} \end{bmatrix}^T \quad (22)$$

$$u_{fdq_k} = \begin{bmatrix} g_{dq_k} & v_{dq_k} \end{bmatrix}^T, \text{ where } g_{dq_k} = u_{dq_{k-1}} \quad (23)$$

$$G_f = L^{-1}\{(sI - A)^{-1}\}\big|_{t=T_s}, \text{ where } A = \begin{bmatrix} -\frac{R_f}{L_f} & \omega \\ -\omega & -\frac{R_f}{L_f} \end{bmatrix} \quad (24)$$

$$S_f = \begin{bmatrix} A^{-1}\left(e^{AT_s} - I\right)B_1 & A^{-1}\left(e^{AT_s} - I\right)B_2 \end{bmatrix}, \text{ where}$$

$$B_1 = \begin{bmatrix} -\frac{R_f}{L_f} & \omega \\ -\omega & -\frac{R_f}{L_f} \end{bmatrix}, B_2 = \begin{bmatrix} \frac{v_{dc}}{L_f} & 0 \\ 0 & \frac{v_{dc}}{L_f} \end{bmatrix} \quad (25)$$

$$C_f = C, \text{ where } C = \begin{bmatrix} 1 & 0 \\ 0 & 1 \end{bmatrix} \quad (26)$$

The values of matrices A, B_1, B_2 and C prescribed in eq (24), (25) and (26) are associated with the continuous state space model of SAPF [7].

The state estimation by KF is formulated in two steps [16] namely predictive and update. In the predictive step, $\hat{x}_{fdq_{k+1|k}}$ is determined from $\hat{x}_{fdq_{k|k}}$.

$$P_{f_{k+1|k}} = G_f P_{f_{k-1}} G_f^{\ T} + W_f \quad (27)$$

$$\hat{x}_{fdq_{k+1|k}} = G_f \hat{x}_{fdq_k} + G_f u_{fdq_k} \quad (28)$$

After measuring the output y_{fdq_k} , the update step corrects the prior estimate-covariance pair $\left(\hat{x}_{fdq_{k+1|k}}, P_{f_{k+1|k}}\right)$ giving a posterior estimate-covariance pair $\left(\hat{x}_{fdq_{k+1|k+1}}, P_{f_{k+1|k+1}}\right)$. The update equations are represented below.

$$P_{f_{k+1|k+1}} = \left(\left(P_{f_{k+1|k}}\right)^{-1} + C_f V_f^{-1} C_f\right)^{-1} \quad (29)$$

$$\hat{x}_{fdq_{k+1|k+1}} = \hat{x}_{fdq_{k+1|k}} - P_{f_{k+1}} C_f^{\ T} V_f^{-1}\left(C_f \hat{x}_{fdq_{k+1|k}} - y_{fdq_k}\right) \quad (30)$$

c. Design of Optimal State Feedback Controller

For full state feedback control design, LQR design seeks to minimize the total transfer of energy from system input to output. The associated Riccati equation solution provides the optimal state feedback controller (K_{LQR}) that can minimize the cost function of the closed loop system given below.

This article has been accepted for publication in a future issue of this journal, but has not been fully edited. Content may change prior to final publication. Citation information: DOI 10.1109/TPEL.2015.2456155, IEEE Transactions on Power Electronics

$$J = \frac{1}{2}\sum_{k=0}^{\infty}\{x_{fdq_k}^{T} Q_L x_{fdq_k} + u_{dq_k}^{T} R_L u_{dq_k}\} \quad (31)$$

where Q_L is a positive semi definite matrix (state weighting matrix) and R_L is a positive definite matrix (control weighting matrix). The entries of matrices Q_L and R_L are chosen such that fastest dynamic response in SAPF system can be achieved.

d. Formulation of Proposed LQG Servo controller

The proposed LQG servo controller ensures that the filter output current of SAPF (i_{fdq}) tracks the reference command (i_{fdq}^{*}) while rejecting process disturbances and measurement noise. The servo controller is the combination of optimal Kalman estimator and optimal state feedback controller and both designs are solved separately, based on the "separation principle".

The extended state space model of the proposed LQG servo controller equations according to (Fig. 2(b)) is given below:

$$x_{servo_{k+1}} = A_{servo} x_{servo_k} + B_{servo} u_{dq_k} \quad (32)$$

$$y_{servo_k} = C_{servo} x_{servo_k} \quad (33)$$

$$u_{dq_k} = -K_m x_{servo_k} \quad (34)$$

where

$$x_{servo_k} = \begin{bmatrix} i_{fd_k} & i_{fq_k} & g_{d_k} & g_{q_k} & \delta_{d_k} & \delta_{q_k} \end{bmatrix}^{T} \quad (35)$$

$$A_{servo} = \begin{bmatrix} A_L & \vdots & 0 \\ \cdots & \vdots & \cdots \\ -C_L A_L & \vdots & 1 \end{bmatrix},$$

$$A_L = \begin{bmatrix} G_f & \vdots & S_f \\ \cdots & \vdots & \cdots \\ 0 & \vdots & 0 \end{bmatrix}, \quad C_L = \begin{bmatrix} 1 & 0 & 0 & 0 \\ 0 & 1 & 0 & 0 \end{bmatrix} \quad (36)$$

$$B_{servo} = \begin{bmatrix} B_L \\ \cdots \\ -C_L B_L \end{bmatrix}, \quad B_L = \begin{bmatrix} 0 & 0 & 1 & 1 \end{bmatrix}^{T} \quad (37)$$

$$C_{servo} = \begin{bmatrix} C_L & \vdots & 0 \end{bmatrix} \quad (38)$$

$$K_m = \begin{bmatrix} K_{LQR} & \vdots & -K_{LQI} \end{bmatrix} \quad (39)$$

K_{LQI} and K_{LQR} are the linear quadratic integrator and linear quadratic regulator gains of the proposed LQG Servo controller respectively and the values of above gains can be achieved from the solutions of the state space model of LQG Servo controller.

IV. RESULTS AND DISCUSSIONS

a. Simulation Results

A simulation model for the three phase SAPF with same parameters shown in Table-I has been developed using MATLAB-Simulink. The proposed LQG servo controller algorithm was implemented using an Embedded MATLAB-Function block that allows simulation of a discrete model that can be easily implemented in a real-time interface (RTI) on the dSPACE1104 R&D control board. A triangular carrier based PWM method is employed for driving three phase IGBT inverter.

For the LQR design, weighting matrices Q_L and R_L are used considering the conventional model of eq (21) extended to include different elements inside the state vector of eq (35). For simplicity, Q_L and R_L are chosen as $Q_L = \mathrm{diag}\{q_1, q_2, q_3, q_4, q_5, q_6\}$ and $R_L = \mathrm{diag}\{r_1, r_2\}$. Since, the output currents (i_{fd}, i_{fq}) of SAPF appear to behave similarly, they should have accompanied with similar weights. Low or close to zero weighting may be placed on these states. But, for effective reactive power compensation through SAPF, the quadrature component (i_{fq}) should be little higher than in-phase component (i_{fd}) i.e., $q_1 \le q_2$. Further, the states associated with the computational delays (g_d, g_q) are actually constrained given other states and hence they are assumed to be zero, i.e., $q_3 = q_4 = 0$. Taking into previous considerations and system symmetry, we have to choose $q_5 \le q_6$ and also a fairly high weighting closer to one should be placed on the output of the feedback compensator in order to attain high bandwidth. We also need to consider the control effort limitation of u_d and u_q, which should be within [-1, +1]. Since R_L is considered to be more than Q_L to avoid large tracking error, we select, $r_1 = r_2 = 1$. Taking into above considerations, several choices for q_1, q_2, q_5 and q_6 have been used for analyzing the behavior of SAPF, (Case-A: $q_1 = 0.000001,\ q_2 = 0.000003,\ q_5 = 0.75,\ q_6 = 0.79$; Case-B: $q_1 = 0.0031,\ q_2 = 0.0035,\ q_5 = 0.91,\ q_6 = 0.93$; Case-C: $q_1 = 0.043,\ q_2 = 0.045,\ q_5 = 0.94,\ q_6 = 0.96$; Case-D: $q_1 = 0.63,\ q_2 = 0.65,\ q_5 = 0.95,\ q_6 = 0.99$). It is seen by trial and error that with the choice of Case-B, the step response of the proposed LQG Servo control system is quite satisfactory as depicted in Fig. 3, where settling time is found to be 3 ms. Thus, Q_L and R_L are expressed by the following eq (40).

$$Q_L = \begin{bmatrix} 0.0031 & 0 & 0 & 0 & 0 & 0 \\ 0 & 0.0035 & 0 & 0 & 0 & 0 \\ 0 & 0 & 0 & 0 & 0 & 0 \\ 0 & 0 & 0 & 0 & 0 & 0 \\ 0 & 0 & 0 & 0 & 0.91 & 0 \\ 0 & 0 & 0 & 0 & 0 & 0.93 \end{bmatrix}, \ R_L = \begin{bmatrix} 1 & 0 \\ 0 & 1 \end{bmatrix} \quad (40)$$

For KF design in reference current estimation, $Q_m = 0.01\, I_{22} A^2$ and $R_m = 20 A^2$ were chosen initially to tune KF in simulation. Further, the weighting signal is minimized more with increase of weighting parameter. Hence, the simulation process is continued by increasing the above covariance values until an optimality of KF can be enriched. After several iteration processes, Q_m and R_m are set to $0.05\, I_{22} A^2$ and $200 A^2$. Similarly, W_f and V_f are set to $0.1\, I_{22} A^2$ and $300 A^2$ respectively for KF implementation in LQG Servo controller.

The simulation results obtained with the proposed SAPF are shown in Fig. 4 considering two Cases (Case-1: Steady-State

This article has been accepted for publication in a future issue of this journal, but has not been fully edited. Content may change prior to final publication. Citation information: DOI 10.1109/TPEL.2015.2456155, IEEE Transactions on Power Electronics

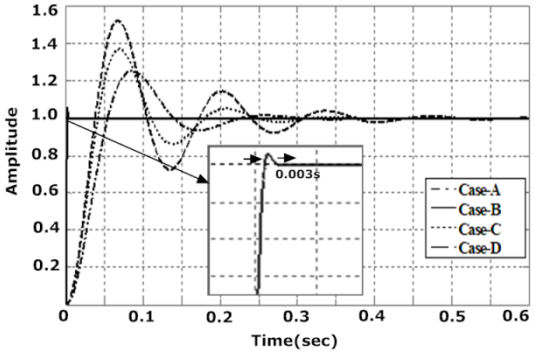

Fig.3 Step Response of the LQG Servo control system with different matrices of Q_L

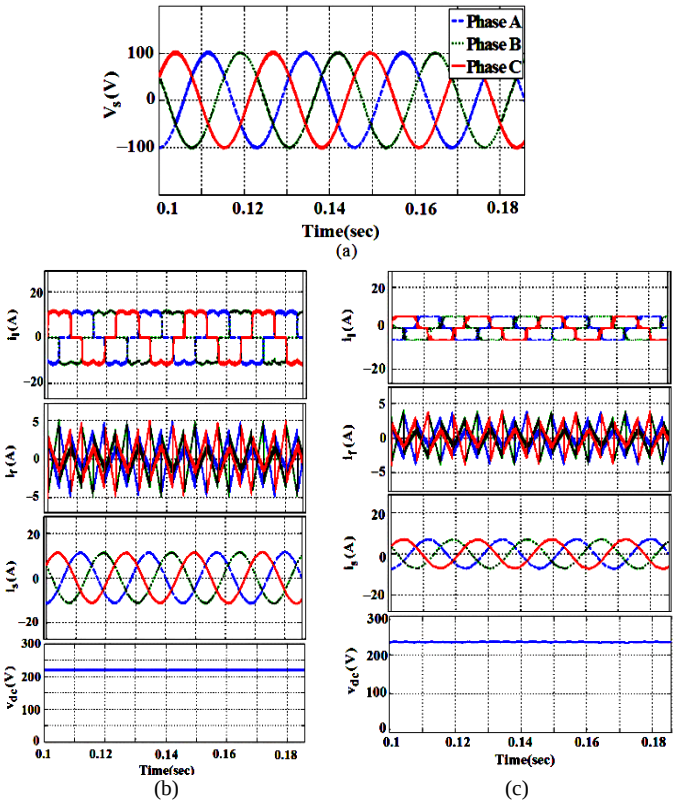

Fig.4 Simulation Results: (a) Waveforms of Balanced Supply voltages, (b) Response of Proposed SAPF in Case-1, (c) Response of Proposed SAPF in Case-2

Load Condition; Case-2: Load impedances are increased by 50%). The supply voltage waveforms are shown in Fig. 4(a). Fig.4 (b) presents the steady state performance of SAPF when the load impedances are kept at the base value (100%). The load current, compensating current, source current and the capacitor voltage are shown for three phases in top to bottom order. The compensated source currents are found to be sinusoidal.

Similar results are found for Case-2 as seen in the respective graphs shown in Fig. 4 (c). The robustness of proposed SAPF is analyzed here. The harmonics distortion results of the source current for phase 'a' before compensation and after compensation with proposed SAPF in both cases are given in Table II. In Case-1, the source current THD is reduced from 25.67% to 3.18%. When load impedance is increased by 50%, the THD is reduced from 21.44% to 2.59% and also the harmonics compensation ratio (HCR) is differed by only 0.27%. Therefore, THDs of the source current are unaffected by the parametric variations of the load. This shows the robustness of proposed SAPF under parametric variations of the load. The HCR factor is calculated as follows:

$$\text{HCR} = \frac{\text{THD\% After Compensation}}{\text{THD\% Before Compensation}} \times 100\% \qquad (41)$$

TABLE II
HARMONICS COMPENSATION EFFECT OF THE PROPOSED LQG Servo_{KF} BASED SAPF (SIMULATION)

Cases	THD% of Phase-a Source Current		
	Before Compensation THD (%)	After Compensation THD (%)	Harmonics Compensation Ratio (HCR) (%)
Case-1	25.67	3.18	12.38
Case-2	21.44	2.59	12.11

b. Experimental Results

The proposed control algorithm has been implemented in real-time on the hardware set up developed in our Lab. A photograph of the experimental setup is shown in Fig.1 (b). The efficacy of the proposed scheme is compared with the existing method (LQR_{KF}) [7], where LQR is employed as current controller and KF for reference current generation in SAPF. The experimental studies for both steady state and dynamic conditions are performed and discussed in the following sections.

Case 1: Balanced Supply Voltages-Steady-State Load Condition

The performance of proposed SAPF is analyzed with the base case load impedance. A diode bridge rectifier with a resistive-inductive load is chosen as the test load to study the operation of SAPF for load compensation. The three phase unit templates (u_a, u_b, u_c) estimated by KF are shown in Fig. 5(a). It is seen that unit templates are undistorted and sinusoidal. Fig. 5(b) and (c) show the load currents (i_{la}, i_{lb}, i_{lc}) and compensating currents (i_{fa}, i_{fb}, i_{fc}) in phase a, b and c respectively. The overall performance of the proposed LQG Servo_{KF} based SAPF is shown in Fig. 5(d). The waveforms shown in this figure are phase-a source voltage, compensating current, source current and dc bus voltage. The source current is found to be almost sinusoidal. The reference tracking behavior of the compensating current for both the proposed and existing method is presented in Fig. 6a (i) and (ii) respectively. It is observed that a tracking delay of "1 ms" is arisen in existing one, whereas it is zero for the proposed method resulting towards an excellent tracking behavior of LQG Servo_{KF} based SAPF system. Further, the waveforms of the source current are shown with start-on condition for the proposed as well as existing method (Fig. 6b (i) and (ii)). The source currents in case of proposed approach are observed to be smooth and distortion less as compared to the existing method. The harmonic spectra are analyzed using a power quality analyzer and the recorded harmonic spectra for uncompensated as well as compensated phase 'a' current are

This article has been accepted for publication in a future issue of this journal, but has not been fully edited. Content may change prior to final publication. Citation information: DOI 10.1109/TPEL.2015.2456155, IEEE Transactions on Power Electronics

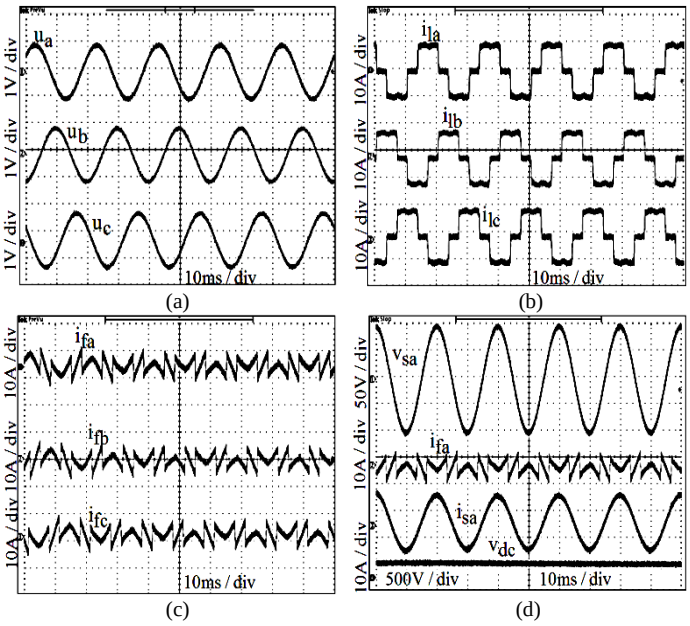

Fig. 5 Case-1: (a) Unit voltage Templates, (b) Three Phase load currents, (c) Three Phase compensating currents in Proposed Method, (d) Phase-a quantities in Proposed Method

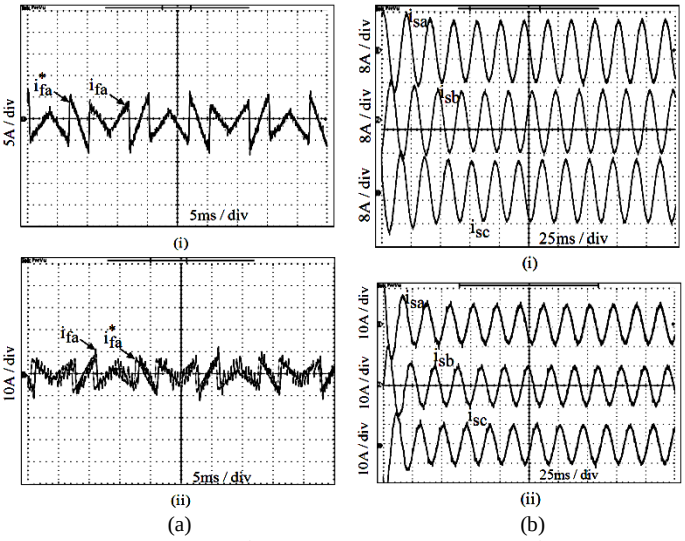

Fig. 6 Case-1: (a) Waveform showing tracking behavior of compensating current, (b) Waveforms of three phase source currents (with Start-on condition), (i) Proposed Method, (ii) Existing Method

shown in Fig. 7. The THD in the load current is as high as 25.9%, but the THD in the source current has been lowered to 3.3% and 4.1% in case of proposed and existing method respectively. Hence it can be concluded that the proposed LQG Servo$_{KF}$ based SAPF provides better reduction in %THD as a requirement set by IEEE519 standard.

Case 2: Balanced Supply Voltages -Load Impedances are increased by 50%:

In this case, the load impedances have been increased by 50% from the base case without alternating any other parameters of the system. Fig. 8(a) shows the three phase load currents, where the amplitude is reduced by 4A as compared to Case-1. Fig. 8(b) shows the compensation characteristics of the proposed SAPF. The source voltage is kept at 100V and the dc link voltage is maintained at 220V. Fig. 8(c) shows the

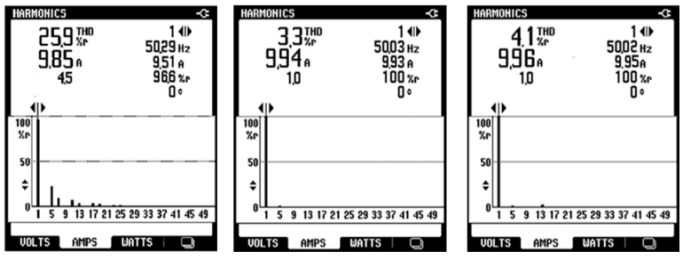

Fig.7 Case-1: Harmonic spectra of (a) phase-a load current, (b) phase-a source current in Proposed Method, (c) phase-a source current in Existing Method

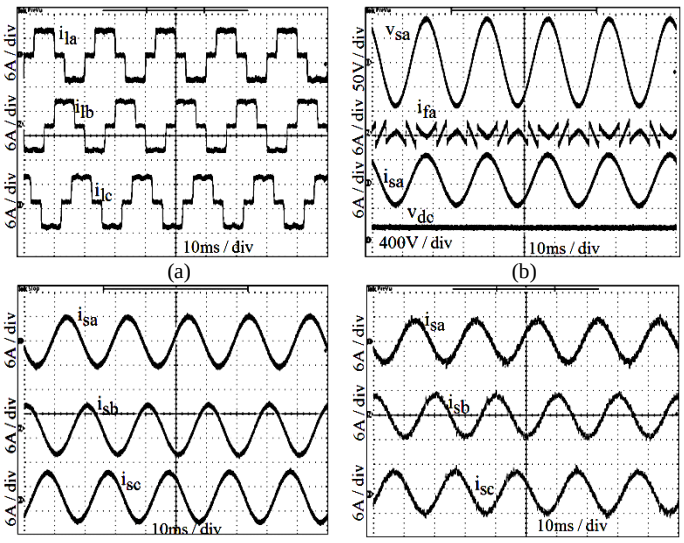

Fig. 8 Case-2: (a) Three Phase load currents, (b) Phase-a quantities in Proposed Method, (c) Three Phase source currents in Proposed Method, (d) Three Phase source currents in Existing Method

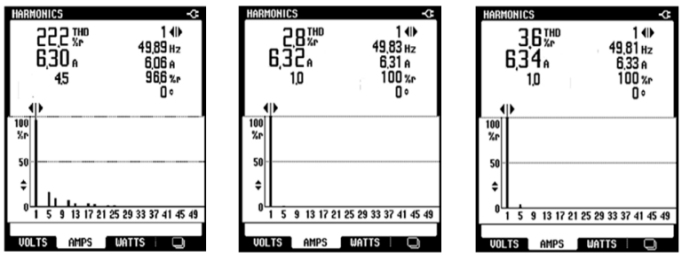

Fig.9 Case-2: Harmonics spectra of (a) phase-a load current, (b) phase-a source current in Proposed Method, and (c) phase-a source current in Existing Method

three phase source currents which are all balanced (≈6.32A) and sinusoidal in the proposed SAPF, however distortions are observed in case of existing method as depicted in Fig. 8(d). The harmonic spectra for load and source current are specified in Fig. 9 employing above two methods. The THD of the load current is reduced from 22.2% to an extent of 2.8% in case of proposed method whereas it is reduced to 3.6% in case of existing method. It is observed that even under parametric variations of load, the proposed control scheme behaves better than existing control strategy.

Case 3: Balanced Supply Voltages -Changing SAPF parameters:

In this case, the SAPF parameters are increased from $R_f = 0.05\Omega, L_f = 2.5\text{mH}$ to $R_f = 0.5\Omega, L_f = 3\text{mH}$. Under

This article has been accepted for publication in a future issue of this journal, but has not been fully edited. Content may change prior to final publication. Citation information: DOI 10.1109/TPEL.2015.2456155, IEEE Transactions on Power Electronics

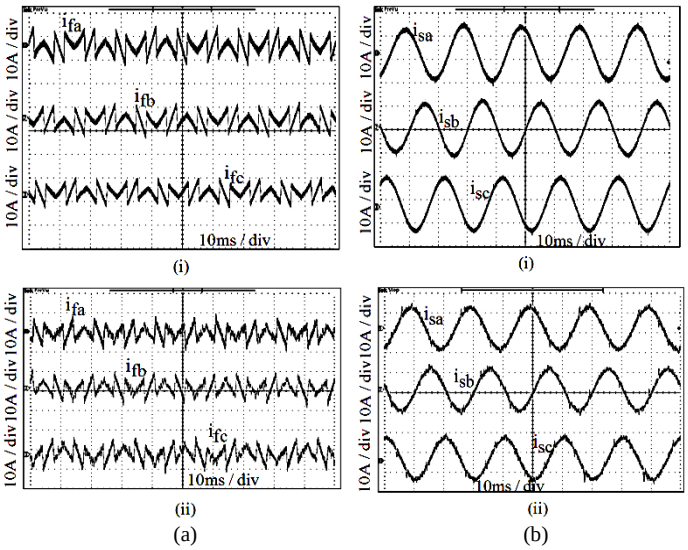

Fig. 10 Case-3: (a) Three phase compensating currents, (b) Three phase source currents , (i) Proposed Method, (ii) Existing Method

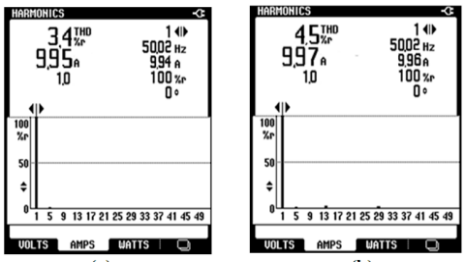

Fig.11 Case-3: Harmonics spectra of (a) phase-a source current in Proposed Method, and (b) phase-a source current in Existing Method

this condition, the performance of the proposed control algorithm is verified with existing technique through Figs. 10-11. It is seen that in case of proposed approach the waveforms for compensating current and the source current are smooth and distortion less as compared to the existing LQR_{KF} method. Hence, the effective harmonics compensation is more in case of proposed $\text{LQG Servo}_{\text{KF}}$ method. Also, the THD of phase-a source current after compensation is analyzed in Fig. 11, which shows the superiority of proposed method (i.e., THD=3.4%) over existing method (i.e., THD=4.5%).

Case 4: Balanced Supply Voltages –Dynamic Load Condition:

The performance of the proposed SAPF, considering the balanced supply voltages, during a sudden load change condition is illustrated in Fig. 12(a). To create dynamic condition, the load is changed from $(\text{R} = 30\Omega, \text{L} = 15\text{mH})$ to $(\text{R} = 20\Omega, \text{L} = 10\text{mH})$. As soon as the load is changed, the compensating current quickly responds to changes to compensate the harmonic currents in the load, as shown in Fig. 12 (b). Also the compensated source current profiles can be viewed from Fig. 12(c) for both existing and proposed techniques. As noticed, the SAPF system with proposed $\text{LQG Servo}_{\text{KF}}$ approach achieves better compensation waveforms as compared to LQR_{KF}. Furthermore, the dc-link voltage in case of existing method settles to the reference

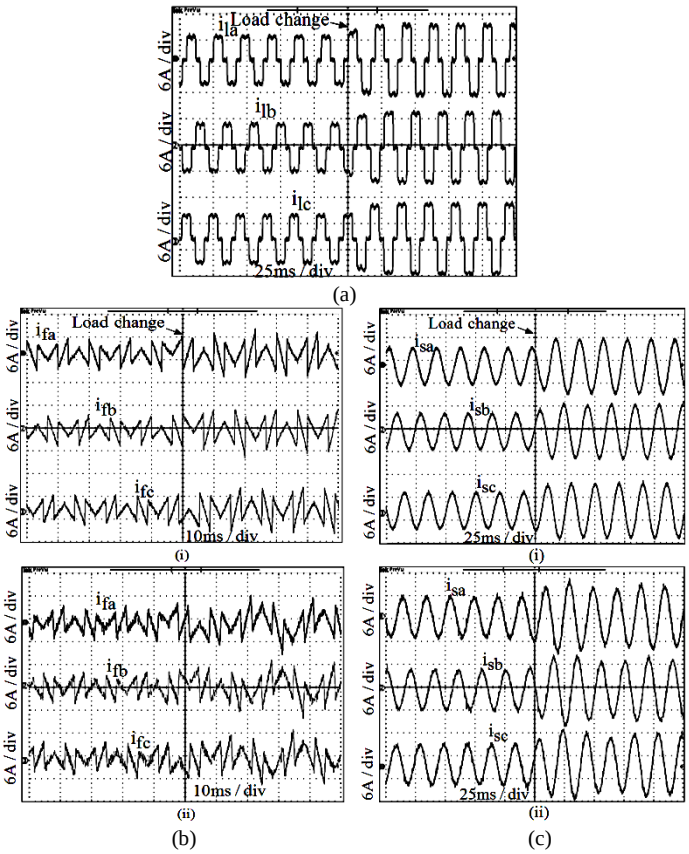

Fig. 12 Case-4: (a) Three phase load currents, (b) Three phase compensating currents, (c) Three phase source currents (i) Proposed Method, (ii) Existing Method

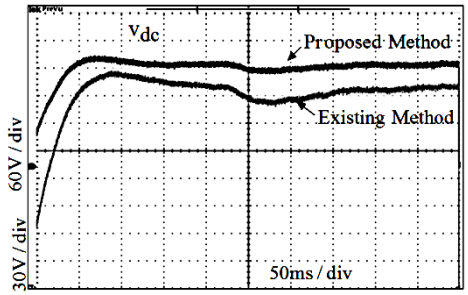

Fig. 13 Case -4: Waveforms of capacitor voltages in Proposed and Existing Method

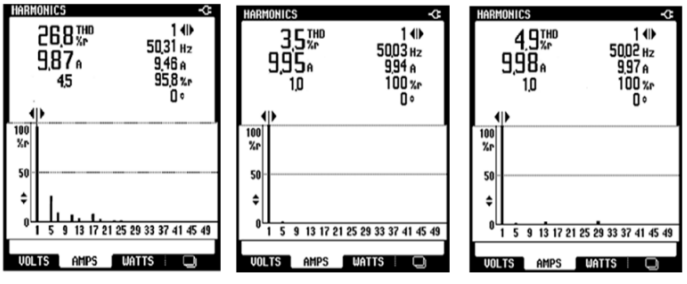

Fig. 14 Case-4: Harmonics spectra of (a) phase-a load current, (b) phase-a source current in Proposed Method, and (c) phase-a source current in Existing Method

value with a time delay of 0.1 sec, while a delay of only 0.025 sec is created for the proposed method as illustrated in Fig. 13. Fig. 14 shows that the supply current THD is effectively reduced from 26.8% to 3.5% and 4.9% in the proposed and

This article has been accepted for publication in a future issue of this journal, but has not been fully edited. Content may change prior to final publication. Citation information: DOI 10.1109/TPEL.2015.2456155, IEEE Transactions on Power Electronics

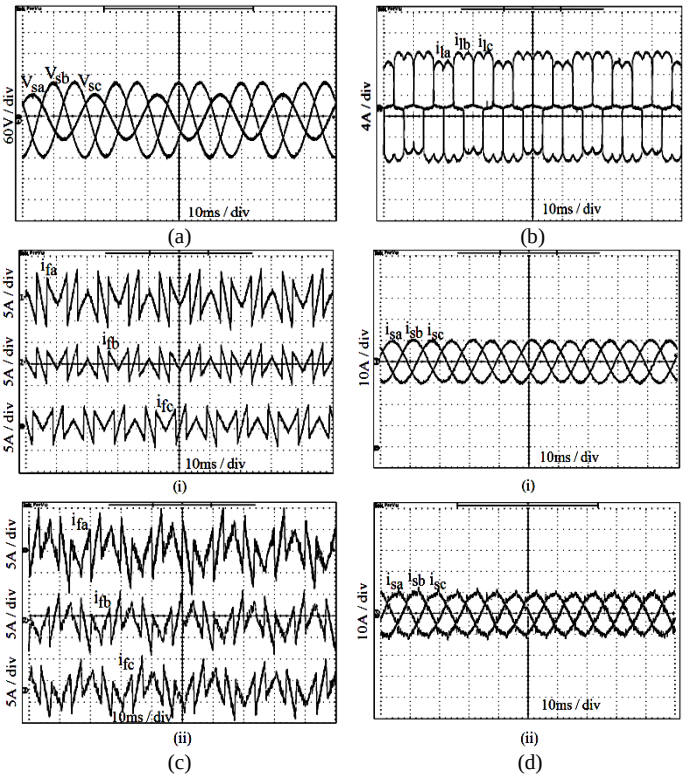

Fig. 15 Case -5: (a) Three phase supply voltages, (b) Three phase load currents, (c) Three phase compensating currents, (b) Three phase source currents ,(i) Proposed Method, (ii) Existing Method

existing method respectively. Thus, this dynamic condition demonstrates the true capability and enhanced performance of proposed LQG Servo_{KF} algorithm over LQR_{KF} based approach.

Case 5: Unbalanced Supply Voltages–Steady-State Load Condition:

In majority of previous Cases, the supply voltage has usually been assumed to be sinusoidal and balanced, but this voltage condition is rare in practical networks. The unbalanced supply voltage condition in practical networks may adversely affect the control performance of the SAPF. To verify the effectiveness of the proposed control algorithm under such condition, experiments were carried out. The profiles for three phase supply voltages and load currents are given in Fig. 15 (a) and (b). To create unbalance, three sensors are required for three phases and phase-a voltage is reduced by 40V as depicted in Fig. 15(a). As a result, phase-a compensating current is increased more to counteract the unbalance as shown in Fig. 15(c). However, the shapes of the compensating current waveforms are smoother in case of proposed algorithm. As shown in Fig. 15(d), the harmonic compensation performance of the SAPF is not deteriorated at unbalanced supply voltage condition and the supply currents are balanced. But, a number of spikes are observed in case of existing method. Furthermore, the dc-link voltage, as shown in Fig. 16, is effectively regulated at the set reference value by employing the proposed LQG Servo_{KF} method. From THD factor analysis for phase-a source current shown in Fig. 17, the proposed method has lower THD (i.e. 3.1%) as compared to

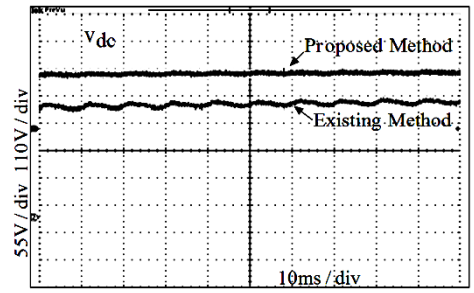

Fig. 16 Case -5: Waveforms of capacitor voltages in Proposed and Existing Method

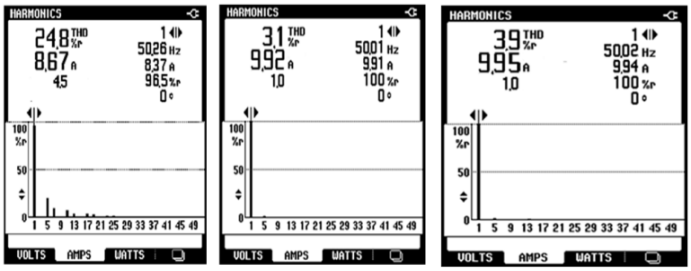

(a) (b) (c)

Fig. 17 Case-5: Harmonics spectra of (a) phase-a load current, (b) phase-a source current in Proposed Method, and (c) phase-a source current in Existing Method

TABLE III
HARMONICS COMPENSATION EFFECT OF THE PROPOSED AND EXISTING CONTROL STRATEGY IN SAPF (EXPERIMENTAL)

Cases	Methods Used in SAPF	THD% of Phase-a Source Current		HCR (%)
		Before Compensation THD (%)	After Compensation THD (%)	
Case1	LQG Servo_{KF}	25.9	3.3	12.74
	LQR_{KF}	25.9	4.1	15.83
Case2	LQG Servo_{KF}	22.2	2.8	12.61
	LQR_{KF}	22.2	3.6	16.21
Case3	LQG Servo_{KF}	25.9	3.4	13.12
	LQR_{KF}	25.9	4.5	17.37
Case4	LQG Servo_{KF}	26.8	3.5	13.05
	LQR_{KF}	26.8	4.9	18.28
Case5	LQG Servo_{KF}	24.8	3.1	12.5
	LQR_{KF}	24.8	3.9	15.76

existing LQR_{KF} (i.e., 3.9%), whereas the load current is distorted with a THD factor of 24.8%.

It is verified through experiments that the proposed LQG Servo_{KF} based SAPF has better steady-state performances as well as better dynamic responses as compared to existing approach. In addition, to evaluate the robustness performance of the existing LQR_{KF} controller and the proposed LQG Servo_{KF} controller considering above five Cases, HCR factors are calculated and summarized in Table III. The results in Table III demonstrate that in case of proposed approach, HCR factors are maintained nearly same (i.e. close to 13%) and these factors are unaffected by any perturbations raised in load or source sides, which makes SAPF system more robust. In contrast, such robustness can't

This article has been accepted for publication in a future issue of this journal, but has not been fully edited. Content may change prior to final publication. Citation information: DOI 10.1109/TPEL.2015.2456155, IEEE Transactions on Power Electronics

be achieved by using existing control strategy, in which HCR factor is largely deviated (i.e. a deviation of 3%) in presence of transient behavior of the load. Thus, the superiority of the proposed algorithm over existing LQR_{KF} is highlighted through all situations of power system perturbations.

V. CONCLUSIONS

We presented a robust LQG Servo controller design for a SAPF. The robustness of the proposed LQG Servo controller strategy has been verified by analyzing the performance under steady state as well as dynamic condition of power system. From the obtained simulation as well as experimental results, the proposed SAPF has been observed to provide efficient current harmonics mitigation, reference current tracking behavior and reactive power compensation with dynamically changing load conditions (other LQR-based approaches are limited to steady-state conditions). The satisfactory experimental results for steady state as well as dynamic conditions demonstrate the feasibility of the proposed algorithm for practical implementation.

In the presence of an additive white Gaussian noise, switching noise, and distortion at PCC voltage, Kalman filter is found to be the best option involving both in reference generation and current controller realization of SAPF. The proposed reference scheme acts as a self-regulator of dc-link voltage escaping from external linear and nonlinear controller and hence an inexpensive control strategy can be implemented. Furthermore, the main feature of the LQG Servo controller is the feedback compensator, which has effects of reducing tracking error distortion, noise and hence a perfect gain stability of SAPF system is achieved. Therefore, the proposed control scheme can be an effective solution for SAPF that requires integrated functionalities.

REFERENCES

[1] Z. Zheng, Y. Huan, T. Shengqing, and Z. Rongxiang , "Objective-Oriented Power Quality Compensation of Multifunctional Grid-Tied Inverters and Its Application in Microgrids," *IEEE Trans. on Power Electron.*, vol. 30, no. 3, pp. 1255-1265, Mar. 2015.

[2] D. Divan, R. Moghe, and A. Prasai, "Power Electronics at the Grid Edge: The key to unlocking value from the smart grid," *IEEE Power Electron. Mag.*, vol. 1, no. 4, pp. 16-22, Dec. 2014.

[3] M. Ali, E. Laboure, and F. Costa, "Integrated Active Filter for Differential-Mode Noise Suppression," *IEEE Trans. on Power Electron.*, vol. 29, no. 3, pp. 1053-1057, Mar. 2014.

[4] R. L. A. Ribeiro, C. C. Azevedo, and R. M. Sousa, "A robust adaptive control strategy of active power filters for power-factor correction, harmonic compensation, and balancing of nonlinear loads," *IEEE Trans. on Power Electron.*, vol. 27, no. 2, pp. 718-730, Feb. 2012.

[5] B. Singh, and J. Solanki, "An implementation of an adaptive control algorithm for a three phase shunt active filter," *IEEE Trans. on Ind. Electron.*, vol. 56, no. 8, pp. 2811-2820, Aug. 2009.

[6] B. Kedjar and K. Al-Haddad, "DSP-based implementation of an LQR with integral action for a three phase three wire shunt active power filter," *IEEE Trans. on Ind. Electron.*, vol. 56, no. 8, pp. 2821-2828, Aug. 2009.

[7] M. Kanieski, R. Cardoso, H. Pinheiro, and H. A. Grundling, "Kalman filter based control system for power quality conditioning devices," *IEEE Trans. on Ind. Electron.*, vol. 60, no. 11, pp. 5214-5227, Nov. 2013.

[8] F. Huerta, D. Pizarro, S. Cobreces, F. J. Rodriguez, C. Giron, and A. Rodriguez, "LQG servo controller for the current control of LCL grid connected voltage source converters," *IEEE Trans. on Ind. Electron.*, vol. 59, no. 11, pp. 4272-4284, Nov. 2012.

[9] W. H. Choi, C. S. Lam, M. C. Wong and Y. D. Han, "Analysis of dc-link voltage controls in three-phase four-wire hybrid active power filters," *IEEE Trans. on Power Electron.*, vol. 28, no. 5, pp. 2180-2191, May 2013.

[10] J. F. Petit, G. Robles, and H. Amaris, "Current Reference Control for Shunt Active Power Filters Under Non sinusoidal Voltage Conditions," *IEEE Trans. on Power Del.*, vol. 22, no. 4, pp. 2254–2261, Oct. 2007.

[11] S. Hu, Z. Zhang, Y. Li, L. Luo, Y. Cao and C. Rehtanz, "A New Half-Bridge Winding Compensation-Based Power Conditioning System for Electric Railway with LQRI," *IEEE Trans. on Power Electron.*, vol. 29, no.10, pp. 5242-5256, Oct. 2014.

[12] R. Cardoso, R. F. D. Camargo, H. Pinheiro, and H. A. Grunling, "Kalman filter based synchronization methods," *IET Generation, Transmission & Distribution*, vol. 2, no. 4, pp. 542–555, Jul. 2008.

[13] P. K. Ray and B. Subudhi, "Ensemble Kalman Filtering Algorithm applied to Power System Harmonics Estimation," *IEEE Trans. on Instrumentation and Measurement*, vol. 61, no. 12, pp. 3216-3224, 2012.

[14] N. Hoffmann and F. W. Fuchs, "Minimal Invasive Equivalent Grid Impedance Estimation in Inductive-Resistive Power Networks Using Extended Kalman Filter," *IEEE Trans. on Power Electron.*, vol. 29, no. 2, pp. 631-641, Feb. 2014.

[15] R. Panigrahi, B. Subudhi, and P. C. Panda, "Model predictive-based shunt active power filter with a new reference current estimation strategy," *IET Power Electron.*, vol. 8, no. 2, pp. 221-233, Feb. 2015.

[16] B. Teixeira, "Kalman filters [ask the experts]", *IEEE Control Syst. Mag.*, vol. 28, no. 2, pp. 16-18, Apr. 2008.

Rakhee Panigrahi received the B.E. degree in Electrical Engineering from University College of Engineering, Burla, Odisha, India, in 2002, and the M.Tech degree in Electrical Engineering from National Institute of Technology (NIT), Rourkela, India, in 2009. Currently, she is pursuing the Ph.D. degree in the Department of Electrical Engineering, National Institute of Technology (NIT), Rourkela, India. Her research is focused on estimation techniques with application to power quality.

Bidyadhar Subudhi received Bachelor Degree in Electrical Engineering from National Institute of Technology (NIT), Rourkela, India, Master of Technology in Control & Instrumentation from Indian Institute of Technology, Delhi in 1988 and 1994 respectively and PhD degree in Control System Engineering from Univ. of Sheffield in 2003. He was as a postdoctoral research fellow in the Dept. of Electrical & Computer Engg., NUS, Singapore during May-Nov 2005. Currently he is a professor in the Department of Electrical Engineering at NIT Rourkela and coordinator, centre of excellence on renewable energy systems. He is a Senior Member of the IEEE and Fellow IET. His research interests include system identification & adaptive control, networked control system, control of flexible and under water robots, estimation and filtering with application to power system and control of renewable energy systems.

Prafulla Chandra Panda received the B.Sc.,M.Sc., and Ph.D. degrees, all in Electrical Engineering from Sambalpur University, Odisha, India, in the year 1971, 1974 and 1990 respectively. Since 1977, he has been with National Institute of Technology (NIT), Rourkela, India, as a Professor in the Department of Electrical Engineering. He is a senior member of the IEEE. At present, his research interests include power system dynamic stability analysis, power quality and high voltage dc transmission.